

TRANSCRIPTION STRATEGY OF CORONAVIRUSES: FUSION OF NON-CONTIGUOUS
SEQUENCES DURING mRNA SYNTHESIS

Willy Spaan¹, Hajo Delius², Mike A. Skinner³, John Armstrong²,
Peter Rottier¹, Sjef Smeekens¹, Stuart G. Siddell³ & Bernard
van der Zeijst¹

¹Institute of Virology, Veterinary Faculty, State
University, Utrecht, The Netherlands

²European Molecular Biology Laboratory, Heidelberg, FRG

³Institute of Virology, Wuerzburg, FRG

SUMMARY

MHV replicates in the cell cytoplasm and viral genetic information is expressed in infected cells as one genomic sized RNA (mRNA1) and six subgenomic mRNAs. The seven RNAs were assumed to have common 3' ends of the size of RNA7, the smallest RNA. The data reported here, show that this model is too simple and that the mRNAs are composed of a leader and body sequence. Electron microscopic analysis of hybrids formed between single stranded cDNA copied from mRNA7 and genomic RNA or mRNA6 shows that genomic RNA, mRNA6 and mRNA7 have common 5' terminal sequences. Furthermore, nucleotide sequence analysis shows that the nucleotide sequence of the 5' end of mRNA7 diverges from the corresponding region of the genome just upstream from the initiation codon of the nucleocapsid gene. Because the synthesis of each mRNA is inactivated by UV irradiation in proportion to its own length, the subgenomic mRNAs are apparently not produced by the processing of larger RNAs. The available data have to be explained by translocation of the polymerase/leader complex to specific internal positions on the negative strand. In this way the leader and body sequences are joined together by a mechanism completely different from conventional RNA splicing but nevertheless giving the same end result.

INTRODUCTION

Viruses were discovered at the end of the nineteenth century (1,2). In the mean time they have been studied to unravel their structure, replication mechanism and pathogenic properties, but they have also been an extremely valuable tool for the study of gene expression of animal cells. Viruses have played a role in the elucidation of protein processing from larger precursors, capping of mRNAs and gene splicing (3,4,5,6). Another interesting aspect of viruses is, that they are the only group of self replicating organisms using RNA as genetic material. The genes of DNA viruses and even RNA tumour viruses are expressed in a way very similar to their host. RNA viruses on the other hand have developed independent strategies (7), but share many biosynthetic pathways with the host cell making them excellent probes for study of cell processes (8,9,10, Rottier et al., this volume).

Although enormous progress has been made in the study of viruses in the last century, there are still a number of virus families of which the replication strategy is almost, or even completely, unknown. These viruses could have new, undetected, mechanisms of gene expression. Until recently coronaviruses were such a group in spite of their pathogenic properties and resulting economic losses (11). However, in the last few years the basic aspects of coronavirus replication have been elucidated (for reviews see 12,13), and the data presented here demonstrates that their strategy involves mechanisms of viral gene expression which have not been described previously.

Coronaviruses are enveloped positive-stranded RNA viruses. The genome RNA is linear, unsegmented and 15000 to 20000 bases in length. The most studied member of the group is murine hepatitis virus (MHV). MHV replicates in the cell cytoplasm and viral genetic information is expressed in infected cells as one genomic sized and six subgenomic mRNAs. These mRNAs are synthesized in non-equimolar amounts, but in relatively constant proportions throughout infection (14). The template for viral mRNA synthesis is a genomic length negative strand (15).

RNase T1 oligonucleotide analysis of MHV-A59 genomic RNA, size-fractionated 3' coterminal (i.e. poly(A)-selected) fragments of genomic RNA and viral mRNA (14,16,17,18) reveals that the viral mRNAs have a "nested set" structure with 3' coterminal ends and sequences extending for different lengths in a 5' direction. Each subgenomic mRNA is capped and polyadenylated, as is genomic RNA (17), and is translated independently to produce a single protein the size of which corresponds to the coding capacity of the 5' sequences not found in the next smallest mRNA (19,20,21). The T1 oligonucleotide analysis also reveals unique oligonucleotides that do not fit into the "nested set" structure. We have demonstrated

that T1 oligonucleotides 10 and 19 from RNA7 of MHV-A59 (using the nomenclature of Lai et al., 17) are not present in the corresponding 3' end of the genome, suggesting that these oligonucleotides come from a leader sequence which all mRNAs might share (18). Oligonucleotide 10 is apparently identical for each mRNA, but mRNA specific electrophoretic mobility differences have been detected for the second oligonucleotide. It is present as oligonucleotide 19, 19a and 3a in mRNA7, mRNA6 and mRNA5, respectively. Oligonucleotides 19, 19a and 17 have very similar base compositions. The latter oligonucleotide is found in mRNA6 and larger mRNAs, but not in mRNA7 (17). Finally, the mRNAs share at least 5 nucleotides at their 5' end (17). These data can be interpreted in the model shown in Fig.1. In this model sequences present at the 5' end of genomic RNA (mRNA1) are also found at the 5' end of each subgenomic mRNA (these sequences will be referred to as leaders). MHV-A59 oligonucleotide 10 would be entirely encompassed within these sequences. MHV-A59 oligonucleotides 19 and 19a would only partly be encompassed within the leader. Their variation would arise from fusion of the leader sequence with the various bodies of the mRNAs. Oligonucleotide 17 would represent sequences at the 5' end of the mRNA7 body, part of which would be lost during the construction of mRNA7 but not for example mRNA6.

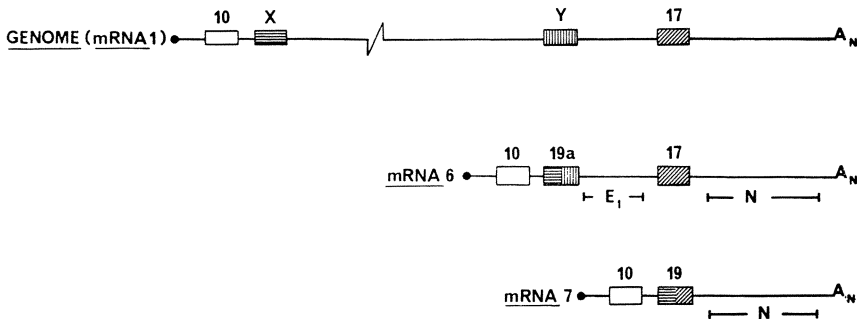


Fig.1. A model for the structural relationships of MHV-A59 genomic RNA and mRNA6 and 7.

The symbols ● and (A)_n represent 5' terminal cap structures and 3' terminal polyadenylate tracts respectively. RNase T1 resistant oligonucleotides are identified by numbers (17). The sequences X and Y have not yet been identified. E₁ (matrix protein) and N (nucleocapsid protein) are the translation products of mRNA6 and mRNA7 respectively. The boxed regions are on a larger scale than the other regions of the mRNAs.

This model is consistent with the available data but lacks experimental evidence. We therefore tested the model by electron microscopic analysis of hybrids formed between cDNA to mRNA7 and genomic RNA or mRNA6. In addition the nucleotide sequence at the 5' end of mRNA7 was compared with the corresponding region of the genome to determine at what point both sequences started to diverge. The above experiments were carried out with MHV-A59. Comparison of the A59 and JHM sequences of mRNA7 was also undertaken. The two viruses have unrelated RNase T1 fingerprints (22) but the recognition sites for the fusion of the leader sequence and the mRNA body can be expected to be conserved.

METHODS

Hybrid duplex mapping

cDNA was prepared as described before (23). The cDNA was incubated with RNA at a concentration of about 1 ug/ml in 50% formamide containing 10 mM Tris-HCl, 1 mM EDTA and 0.2 M CsCl for 30 min at 40°C. A 10-fold diluted aliquot was spread from 30% formamide, 0.1 M Tris-HCl, 1 mM EDTA, 0.1 ug/ml PM2 DNA with CNBr-treated cytochrome (24) on a hypophase of distilled water. Samples were picked up on Parlodion-coated grids, stained with uranyl acetate and rotary shadowed with platinum.

RNA sequencing

For the dideoxy reaction, 2 μ l of the single stranded synthetic DNA primer (Biolabs New England) (10 ng/ μ l) 1 μ l of RNA7 or genomic RNA (1 mg/ml), 2 μ l tenfold concentrated reverse transcriptase buffer (1x buffer is 50 mM Tris-HCl pH 8.3, 50 mM KCl and 8 mM MgCl₂) 8 μ l H₂O, 0.5 μ l of 10 mM DTT, and 3 μ l reverse transcriptase (2 U/ μ l; from W.Beard) were mixed. To 4 μ l of this primed mRNA 1 μ l of one of the following chain-terminating nucleotide stock mixtures were added; ddA mixture: 50 μ M dCTP, 50 μ M dGTP, 50 μ M dTTP and 1 μ M ddATP; ddC mixture: 25 μ M dCTP, 50 μ M dGTP, 50 μ M dTTP and 2.5 μ M ddCTP; ddG mixture: 50 μ M dCTP, 25 μ M dGTP, 50 μ M dTTP and 2.5 μ M ddGTP, ddT mixture: 125 μ M dCTP, 125 μ M dGTP, 125 μ M dTTP and 12.5 μ M ddTTP. All these mixtures contained 4 μ Ci α -³²P dATP (400 Ci.mmol⁻¹). Incubation was at 42°C for 30 min and 1 μ l of a 0.125 mM solution of unlabeled deoxynucleoside triphosphate was then added and the mixture was chased for an additional 0.5 hr. The reaction products were analyzed on 0.25 mm thick and 40 cm long 6% polyacrylamide gels (25). The sequence procedure for clone S9 has been described (23).

RESULTS

Electron microscopy of hybrids between cDNA to RNA7 and genomic RNA or mRNA6

cDNA was prepared as described before (23). After hydrolysis of the RNA template it was treated with glyoxal and dimethylsulfoxide and analyzed by agarose gel electrophoresis. A main band of approximately the size of the RNA7 was seen (data not shown). This cDNA was annealed to genomic RNA and prepared for electron microscopy by cytochrome spreading. A sequence homology between the 5' end of mRNA7 copied into the cDNA, and the 5' end of the genomic RNA should lead to the formation of a looped hybrid. Indeed such structures were observed. Fig.2A shows such a hybrid molecule accompanied by a tracing outlining the possible arrangement of the RNA and DNA strands. No circles but only linear molecules were observed in preparations of RNA alone prepared in the same way, so that the circularization has to be attributed to the hybrid formation. The length of the hybrid region in these molecules corresponds to 1995 ± 160 bp, using PM2 DNA as a standard and after correction for the shortened hybrid length (26). The size of the loop was determined as 19.4 ± 1.0 kb. This value is only an approximation due to lack of a suitable RNA standard of this size. No double strand could be discerned at the point of the re-entry of the genomic RNA into the hybrid near the 5' end. This excludes a double strand region much larger than 50 nucleotides. Fig.2B shows a hybrid between the same cDNA and RNA6. Again, a double-stranded region (1890 ± 140 bp) caused by the hybridization between the cDNA and the 3'-end of mRNA6, and a single-stranded loop structure (but in this case a much smaller one of 600 ± 80 nucleotide) were observed. This single stranded loop probably represents the E1 gene. Its size would be sufficient to code for a polypeptide of 22.0 ± 2.9 K daltons, the approximate size of the non-glycosylated form of polypeptide E1 found in MHV-A59 infected cells (20, Armstrong et al., this volume). Again, the most likely explanation of the loop formation in these hybrids is the presence of common leader sequences in mRNA6 and mRNA7, although again no hybrid stretch on the 5' side of the loop could be detected. The data very strongly support the model given in Fig.1.

Sequence analysis of mRNA7 and the region of the genome between the E1 and N genes

Another prediction of the model is that the nucleotide sequence of the region immediately upstream from the nucleocapsid gene of mRNA7 should diverge from the region upstream from the nucleocapsid gene in the genome. Therefore we determined the nucleotide sequences in these regions.

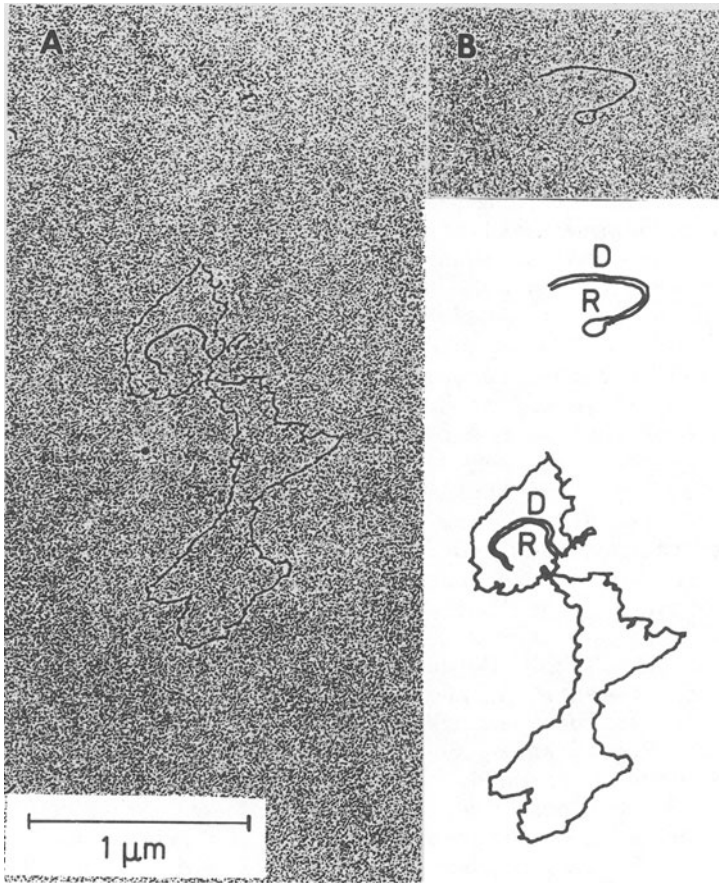


Fig.2. Electron micrographs of hybrids between coronavirus MHV-A59 RNAs and cDNA synthesized on RNA7.

- (A) Hybrid between cDNA and the genomic RNA.
- (B) Hybrid between cDNA and RNA6.

The tracings indicate the hypothetical arrangement of the cDNA (D) and the RNA (R). The structure of the joint between the 5' end of the RNA loops and the cDNA cannot be identified in the electron micrographs. Viral RNAs were isolated as described (18).

Recently we have cloned and sequenced cDNA prepared from MHV-A59 mRNAs (23). A sequence of 1817 nucleotides of the 3' end of the genome, including the nucleocapsid gene was determined by shot-gun sequencing of restriction fragments in phage M13. The approach we have used here was to sequence directly the 5' end of mRNA7 and the corresponding region of the genome of MHV-A59 using

a DNA primer and reverse transcriptase for dideoxy sequencing on RNA (27). The primer was complementary to position 11 to 24 of the nucleocapsid gene sequence (23). A sequence of 86 bases could be read on RNA7 (Fig.3A). The following conclusions can be drawn. First, two large T1 oligonucleotides are predicted from this sequence. One oligonucleotide (position -53/-29) would have a base composition very similar to T1 oligonucleotide 10. The other one (position -25/-2) was very similar to oligonucleotide 19. Second, although the extreme end of RNA7 could not be determined the sequence NAAG at the 5' end is almost identical to the sequence found at the 5' end of MHV-A59 RNAs by Lai et al. (cap - NUAAG) (17). Therefore we assume that the 5' noncoding region (including the leader sequence) of mRNA7 is 78 nucleotides long.

The same DNA primer was used for dideoxy sequencing on the genome. This sequence is shown in Fig. 3B. The sequence starting at position -21 until position -2 is very similar to the predicted sequence of T1 oligonucleotide 17. The T1 oligonucleotides 10 and 19 are not present in this sequence, which is to be expected from the model shown in Fig.1. The sequence preceding T1 oligonucleotide 17 represents the 3' end of the E1 gene. This sequence is in good agreement with the sequence of E1 obtained from cDNA clones (Armstrong et al., this volume). Comparison of the sequence of the 5' terminus of RNA7 and the sequence of the genome shows that both sequences are identical until position -22 (Fig.3C). From this position RNA7 and the genome start to diverge. The divergence site is located at the beginning of T1 oligonucleotide 17 and within T1 oligonucleotide 19.

Localization of the fusion site of leader and body sequences of MHV mRNAs

From the above data, summarized in Fig.4, it is clear that the 5' terminus of the MHV-A59 mRNA7 body cannot extend beyond position -21, the site of divergence of mRNA7 and the genome. As mentioned before T1 oligonucleotide 19a, (specific for RNA6) and T1 oligonucleotide 19 (specific for RNA7) have a very similar base composition. By predicting the sequence of 19a from the base composition and by comparing this sequence to the sequence of mRNA7 between -24 and -2 it can be seen that the 3' terminus of the leader sequence fused to mRNA6 cannot extend beyond the first base difference (reading in a 5' to 3' direction) between oligonucleotide 19 and 19a. Thus the data suggest that for MHV-A59 the fusion of leader and body sequences producing oligonucleotides 19 and 19a occurred within the sequence 5' AAUCUAAUCUAAACU 3', a sequence that does not contain the consensus (A/C) AG/G established for splice junctions in viral and cellular mRNAs (6). This sequence contains two copies of the palindromic pentamer AUCUA (or the pentamer AAUCU). It was surprising that the only major difference between A59 and JHM virus was the presence of a

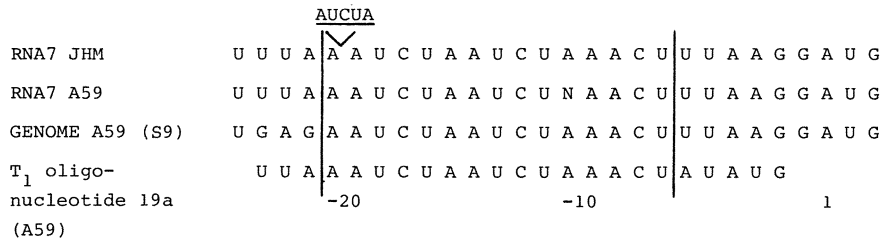


Fig.4. Localization of the fusion site between body and leader of MHV mRNA. For details see text.

third copy of the pentamer AUCUA (or the sequence AAUCU). Despite some differences the sequence homology is extended over the complete noncoding and coding region (Skinner and Siddell, this volume). The presence of a third copy of the palindromic pentamer AUCUA (or the sequence AAUCU) in the MHV-JHM sequence may suggest that it functions as a recognition signal during the fusion process.

DISCUSSION

How are leader and body of coronaviral mRNAs fused?

There is at present no indication that the replication of MHV involves a nuclear phase or nuclear factors. MHV is reported to grow in enucleated cells and its replication is not inhibited by actinomycin D or alpha-amanitin (28,29,30). Also, the synthesis of each mRNA is inactivated by UV irradiation in proportion to its own length (31). Thus the subgenomic mRNAs are apparently not produced by the processing of larger RNAs. These data exclude that conventional splicing mechanisms are involved in MHV mRNA synthesis.

However, the data could be explained by a RNA polymerase jump or translocation during the synthesis of the positive strands. Two possible models are shown in Fig.5. Translocation could occur by formation of stable loop structures in the negative strand (Fig.5A). When the sequence located just upstream from the fusion site is also present downstream of the leader sequence at the 5' end of the genome but in a complementary inverted way a stable loop structure can be formed. In this way the polymerase would translocate through intervening sequences on the negative strand and resume transcription at the beginning of a particular cistron. In the second model the leader acts as a primer at different sites on the negative stranded template (Fig.5B). This mechanism would involve the synthesis of a short RNA transcript from the 3' end of

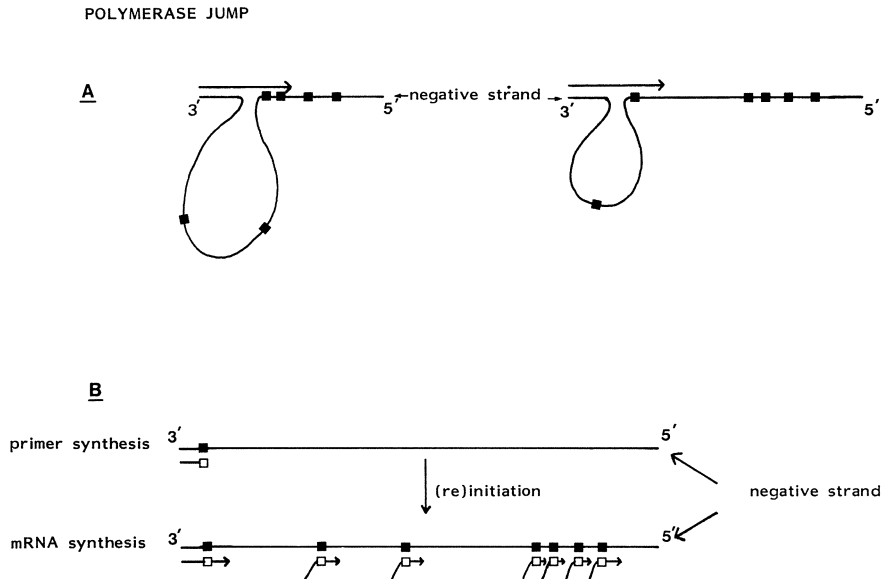


Fig.5. A model for an RNA polymerase jump or translocation mechanism during the synthesis of positive stranded MHV-A59 RNAs.

(A) Formation of stable loop structures

(B) Primed RNA synthesis

The black boxes represent the beginning of a particular cistron.

the negative stranded-*template*. The leader or polymerase/leader complex would then be translocated to an internal position on the negative stranded *template* where transcription would resume. This translocation may or may not involve dissociation of the polymerase/leader complex from the *template*. Translocation would have to occur to specific positions and at specific frequencies. It seems likely that this specificity would be, at least in part, related to sequences in the 5' non-coding region of MHV mRNAs. We have argued that the fusion of leader and body sequences during the synthesis of mRNA7 and mRNA6 occurs within the sequence 5'AAUCUAAUCUAAACU 3'. This sequence or its 5' end might also be present within region X of the leader (Fig.1). Although we have no sequence data of this region X, we assume that T1 oligonucleotide 19, which is also present in a T1 fingerprint of genomic RNA (17,18), is located at this position. Thus the same sequence of 15 nucleotides is present at the 5' end of the genome as at the region just upstream from the nucleocapsid gene. When the synthesis of the primer would terminate within this 15 nucleotides long repeat, a donor and acceptor site sequence homology would be created (Fig.6).

PRIMER BINDING MODEL

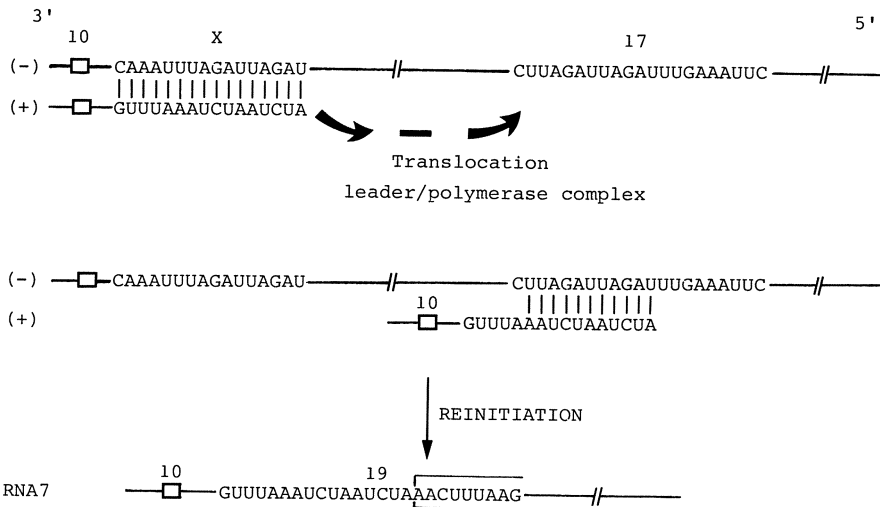


Fig.6. Primer binding model for the synthesis of MHV-A59 mRNA7. In this model the sequence upstream from the initiating ATG is also present in region X of the genome. The synthesis of the leader is terminated in region X and the leader is translocated to the region just upstream from the nucleocapsid gene. Because the 3' end of the leader is complementary to that part of the negative strand equivalent to T1 oligonucleotide 17 it can bind to this region. After (re)initiation of RNA synthesis mRNA7 is made. (The numbers 10, 17 and 19 represent RNase T1 resistant oligonucleotides).

Considering the fact that only one double-stranded replicative form has been found in infected cells (15, Lai et al., this volume) we favor the model depicted in Fig.5B and Fig.6. The mechanism we propose for the generation of coronaviruses would resemble that observed for the formation of DI influenza virus RNA (32). Fields and Winter suggest that after the termination of transcription in a U-rich region of influenza genomic RNA, sequences at the 3' terminus of the nascent chain play a role in the recognition of reinitiation positions downstream on the template.

A similar mechanism might also explain the high frequency of recombination between aphthovirus RNAs (33).

Primed RNA synthesis is furthermore found during the replication of influenza virus. Newly synthesized cellular mRNA sequences are sequestered and used as primers for mRNA synthesis (34). However, because T1 oligonucleotide 10 is labeled in the presence of actinomycin D, the primer involved in the coronavirus mRNA synthesis must be virus-coded rather than transcribed from a host cell gene.

In addition, translocations caused by leaping of the RNA polymerase are thought to cause the generation of defective interfering (DI) particles of RNA viruses. (35,36). Therefore, it could be argued that the way MHV mRNAs are constructed is not unique to coronaviruses, but rather that it represents a refinement of a mechanism which occurs quite generally, in a haphazard way, in cells infected with RNA viruses.

The transcription process has many interesting features that remain to be resolved. How is the transcription regulated so that the mRNAs are synthesized in non-equimolar amounts? How many proteins are involved in the synthesis of the MHV RNAs and where are the recognition signals located on the RNA template(s)? We have determined the sequence of the 5' end of mRNA7 and because this sequence is derived from the 5' end of the genome we now know the sequence of the 3' end of the negative strand. Comparison of this sequence to the 3' end of the genome (23) shows that there is no sequence homology. This suggests that different enzymes with different recognition signals are involved in the synthesis of negative and positive strands. This is in agreement with the finding of two polymerase activities in MHV-A59 infected cells (37) and the identification of five to six complementation groups in complementation analysis of ts-mutants which were defective in their ability to induce virus-specific RNA synthesis (38, Van der Zeijst manuscript in preparation). Clearly, further sequence analysis of the extreme 5' end of the genome and of more intergenic regions are needed to elucidate the details of this unusual mechanism of RNA synthesis.

ACKNOWLEDGMENTS

We thank Maud Maas Geesteranus for preparation of the manuscript. This investigation was supported by the Foundation for Medical Research (FUNGO) (W.S.) and by the Deutsche Forschungsgemeinschaft (M.S. and S.S.). P.R. was supported at the EMBL by a short-term EMBO fellowship and J.A. by a European Fellowship from the Royal Society.

REFERENCES

1. M.W. Beijerinck, *Centralbl. Bacteriol. Parasitenk. Abt. II* 5:27-33 (1899).
2. D.I. Ivanovsky, *Sel.' Khoz. Lêsov.* 169:108-121 (1882).
3. B.E. Butterworth, *Curr.Top.Microbiol.Immunol.* 77:1-41 (1977).
4. A.J. Shatkin, *Curr.Top.Microbiol.Immunol.* 93:1-4 (1981).
5. A.K. Banerjee, *Microbiol. Rev.* 44:175-205 (1980).
6. S.J. Flint, *Curr.Top.Microbiol.Immunol.* 93:47-79 (1981).
7. D. Baltimore, *Bacteriol. Rev.* 35:235-241 (1971).
8. H. Garoff, C. Kondor-Koch, H. Riedel, *Curr.Top.Microbiol. Immunol.* 99:1-50 (1982).
9. H.F. Lodish, W.A. Braell, A.L. Schwartz, G.J.A.M. Strous, and A. Zilberstein, *Int.Rev.Cytol.suppl.* 12:247-307 (1981).
10. M.F.G.Schmidt, *Curr.Top.Microbiol.Immunol.* 102:107-129 (1983).
11. B.W.J. Mahy, *Nature* 288:536-538 (1980).
12. S.G. Siddell, H. Wege, and V. ter Meulen, *J.gen.Virol.* 64:761-776 (1983).
13. L.S. Sturman and K.V. Holmes, *Advances in Virus Research*, 28: in press (1983).
14. J.L. Leibowitz, K.C. Wilhelmsen, and C.W. Bond, *Virology* 114:39-51 (1981).
15. M.M.C. Lai, C.D. Patton, and S.A. Stohlman, *J.Virol.* 44:487-492 (1982).
16. M.M.C. Lai, P.R. Brayton, R.C. Armen, C.D. Patton, C. Pugh, and S.A. Stohlman, *J.Virol.* 39:823-834 (1981).
17. M.M.C. Lai, C.D. Patton, and S.A. Stohlman, *J.Virol.* 41:557-565 (1982).
18. W.J.M. Spaan, P.J.M. Rottier, M.C. Horzinek, and B.A.M. Van der Zeijst, *J.Virol.* 42:432-439 (1982).
19. S.G. Siddell, *J.gen.Virol.* 64:113-125 (1983).
20. P.J.M. Rottier, W.J.M. Spaan, M.C. Horzinek, and B.A.M. Van der Zeijst, *J.Virol.* 38:20-26 (1981).
21. J.L. Leibowitz, S.R. Weiss, E. Paavola and C.W. Bond, *J. Virol.* 43:905-913 (1982).
22. M.M.C. Lai and S.A. Stohlman, *J.Virol.* 38:661-670 (1981).
23. J. Armstrong, S. Smeekens, and P. Rottier, *Nucleic Acids Res.* 11:883-891 (1983).
24. H. Delius, H. Westphal, and N. Axelrod, *J.Molec.Biol.* 74:677-687 (1972).
25. H. Garoff and W. Ansorge, *Analyt.Biochem.* 115:450-457 (1981).
26. H. Priess, B. Koller, B. Hess, and H. Delius, *Molec.gen.Genet.* 178:27-34 (1980).
27. D. Zimmern and P. Kaesberg, *Proc.natn.Acad.Sci.U.S.A.* 75:4257-4261 (1978).
28. P.R. Brayton, R.G. Ganges, and S.A. Stohlman, *J. gen. Virol.* 56:457-460 (1981).
29. K.C. Wilhelmsen, J.L. Leibowitz, C.W. Bond, and J.A. Robb, *Virology* 110:225-230 (1983).

30. B.W.J. Mahy, S. Siddell, H. Wege, and V. Ter Meulen, *J.gen.Virol.* 64:103-111 (1983).
31. L. Jacobs, W.J.M. Spaan, M.C. Horzinek, and B.A.M. Van der Zeijst, *J.Virol.* 39:401-406 (1981).
32. S. Fields and G. Winter, *Cell* 28:303-313 (1982).
33. A.M.W. King, D. McCahon, W.R. Slade, and J.W.I. Newman, *Cell* 29:921-928 (1982).
34. S.J. Plotch, M. Bouloy, I. Ulmanen, and R. Krug, *Cell* 23:847-858 (1981).
35. J. Perrault, *Curr.Topics Microbiol.Immunol.* 93:151-207 (1981).
36. R.D. Lazzarini, J.D. Keene, and M. Schubert, *Cell* 26:145-154 (1981).
37. P.R. Brayton, M.M.C. Lai, C.D. Patton, and S.A. Stohlman, *J.Virol.* 42:847-853 (1982).
38. J.L. Leibowitz, J.R. DeVries, and M.V. Haspel, *J.Virol.* 42:1080-1087 (1982).